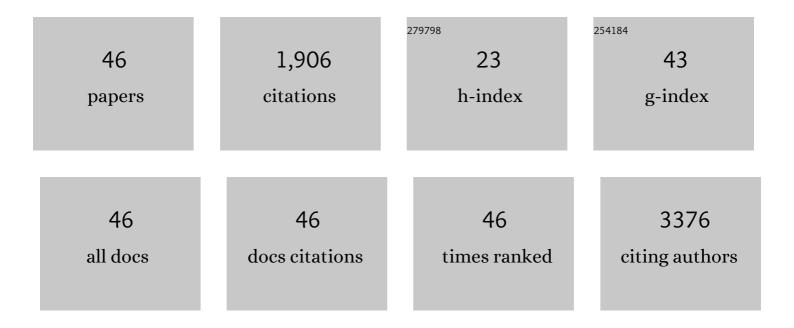
Weifeng Yang

List of Publications by Year in descending order

Source: https://exaly.com/author-pdf/1948960/publications.pdf Version: 2024-02-01



#	Article	IF	CITATIONS
1	Threshold voltage modulation in monolayer MoS2 field-effect transistors via selective gallium ion beam irradiation. Science China Materials, 2022, 65, 741-747.	6.3	5
2	Interfacial properties of 2D WS2 on SiO2 substrate from X-ray photoelectron spectroscopy and first-principles calculations. Frontiers of Physics, 2022, 17, .	5.0	3
3	Determination of band alignments at 2D tungsten disulfide/high-k dielectric oxides interfaces by x-ray photoelectron spectroscopy. Applied Surface Science, 2020, 505, 144521.	6.1	8
4	Far out-of-equilibrium spin populations trigger giant spin injection into atomically thin MoS2. Nature Physics, 2019, 15, 347-351.	16.7	105
5	Surface-engineered cobalt oxide nanowires as multifunctional electrocatalysts for efficient Zn-Air batteries-driven overall water splitting. Energy Storage Materials, 2019, 23, 1-7.	18.0	48
6	Metal–organic framework-derived hierarchical MoS ₂ /CoS ₂ nanotube arrays as pH-universal electrocatalysts for efficient hydrogen evolution. Journal of Materials Chemistry A, 2019, 7, 13339-13346.	10.3	133
7	Angle-shaped triboelectric nanogenerator for harvesting environmental wind energy. Nano Energy, 2019, 56, 269-276.	16.0	127
8	Direct n- to p-Type Channel Conversion in Monolayer/Few-Layer WS ₂ Field-Effect Transistors by Atomic Nitrogen Treatment. ACS Nano, 2018, 12, 2506-2513.	14.6	107
9	A flexible photo-thermoelectric nanogenerator based on MoS2/PU photothermal layer for infrared light harvesting. Nano Energy, 2018, 49, 588-595.	16.0	124
10	Band alignment of 2D WS2/HfO2 interfaces from x-ray photoelectron spectroscopy and first-principles calculations. Applied Physics Letters, 2018, 112, 171604.	3.3	14
11	Simultaneous edge and electronic control of MoS ₂ nanosheets through Fe doping for an efficient oxygen evolution reaction. Nanoscale, 2018, 10, 20113-20119.	5.6	63
12	Interlayer interactions in 2D WS ₂ /MoS ₂ heterostructures monolithically grown by <i>in situ</i> physical vapor deposition. Nanoscale, 2018, 10, 22927-22936.	5.6	62
13	Morphology Transition of ZnO Nanorod Arrays Synthesized by a Two-Step Aqueous Solution Method. Crystals, 2018, 8, 152.	2.2	7
14	Flexible thermoelectric nanogenerator based on the MoS ₂ /graphene nanocomposite and its application for a self-powered temperature sensor. Semiconductor Science and Technology, 2017, 32, 044003.	2.0	47
15	TiNbO ₂ -Based Photodetectors With Low Dark Current and High UV-to-Visible Rejection Ratio. IEEE Photonics Technology Letters, 2016, 28, 837-840.	2.5	2
16	Photon Upconversion Through Tb ³⁺ â€Mediated Interfacial Energy Transfer. Advanced Materials, 2015, 27, 6208-6212.	21.0	89
17	Separated-absorption-multiplication 4H-SiC avalanche photodiodes with adjustable responsivity and response time. Japanese Journal of Applied Physics, 2015, 54, 070303.	1.5	2
18	Pulse laser deposition of epitaxial TiO 2 thin films for high-performance ultraviolet photodetectors. Applied Surface Science, 2015, 355, 398-402.	6.1	24

WEIFENG YANG

#	Article	lF	CITATIONS
19	High-performance 4H-SiC-based p-i-n ultraviolet photodiode and investigation of its capacitance characteristics. Optics Communications, 2014, 333, 182-186.	2.1	33
20	Lanthanide-doped upconversion materials: emerging applications for photovoltaics and photocatalysis. Nanotechnology, 2014, 25, 482001.	2.6	146
21	Development of <scp><scp>ZnO</scp></scp> Nanostructured Films via Sodium Chloride Solution and Investigation of Its Growth Mechanism and Optical Properties. Journal of the American Ceramic Society, 2013, 96, 1972-1977.	3.8	1
22	Low substrate temperature fabrication of high-performance metal oxide thin-film by magnetron sputtering with target self-heating. Applied Physics Letters, 2013, 102, .	3.3	11
23	Enhancement of bandgap emission of Pt-capped MgZnO films: Important role of light extraction versus exciton-plasmon coupling. Optics Express, 2012, 20, 14556.	3.4	16
24	Unexpected improved conductivity and systematic low-temperature anomalies of a new germanium zinc indium oxide system. Europhysics Letters, 2012, 100, 17003.	2.0	1
25	Properties of low indium content Al incorporated IZO (indium zinc oxide) deposited at room temperature. Journal of Applied Physics, 2012, 112, .	2.5	18
26	Temperature-dependent exciton luminescence from an Au-nanopattern–coated ZnCdO film. Europhysics Letters, 2012, 99, 27003.	2.0	6
27	Improvement of GaN light-emitting diodes with surface-treated Al-doped ZnO transparent Ohmic contacts by holographic photonic crystal. Applied Physics A: Materials Science and Processing, 2012, 107, 809-812.	2.3	10
28	Thermal-assisted anisotropy and anisotropy-driven instability in the superfluid state of two-species fermionic polar molecules. Physics Letters, Section A: General, Atomic and Solid State Physics, 2012, 376, 1986-1991.	2.1	0
29	Low-Dark-Current \$hbox{TiO}_{2}\$ MSM UV Photodetectors With Pt Schottky Contacts. IEEE Electron Device Letters, 2011, 32, 530-532.	3.9	39
30	Photoluminescence characteristics of ZnCdO/ZnO single quantum well grown by pulsed laser deposition. Applied Physics Letters, 2011, 98, 121903.	3.3	17
31	Temperature dependence of weak localization effects of excitons in ZnCdO/ZnO single quantum well. Journal of Applied Physics, 2011, 109, .	2.5	19
32	Low dark current metal-semiconductor-metal ultraviolet photodetectors based on sol-gel-derived TiO2 films. Journal of Applied Physics, 2011, 109, .	2.5	36
33	Room temperature deposition of Al-doped ZnO films on quartz substrates by radio-frequency magnetron sputtering and effects of thermal annealing. Thin Solid Films, 2010, 519, 31-36.	1.8	92
34	Deposition of Ni, Ag, and Pt-based Al-doped ZnO double films for the transparent conductive electrodes by RF magnetron sputtering. Applied Surface Science, 2010, 256, 7591-7595.	6.1	12
35	Ultraviolet light emission and excitonic fine structures in ultrathin single-crystalline indium oxide nanowires. Applied Physics Letters, 2010, 96, .	3.3	46
36	Surface-plasmon enhancement of band gap emission from ZnCdO thin films by gold particles. Applied Physics Letters, 2010, 97, 061104.	3.3	18

Weifeng Yang

#	Article	IF	CITATIONS
37	Pulsed laser deposition of high-quality ZnCdO epilayers and ZnCdO/ZnO single quantum well on sapphire substrate. Applied Physics Letters, 2010, 97, 061911.	3.3	34
38	Metal–Semiconductor–Metal Ultraviolet Photodetectors Based on \$hbox{TiO}_{2}\$ Films Deposited by Radio-Frequency Magnetron Sputtering. IEEE Electron Device Letters, 2010, 31, 588-590.	3.9	35
39	Surface plasmon induced exciton redistribution in ZnCdO/ZnO coaxial multiquantum-well nanowires. Applied Physics Letters, 2010, 97, .	3.3	11
40	Room-temperature deposition of transparent conducting Al-doped ZnO films by RF magnetron sputtering method. Applied Surface Science, 2009, 255, 5669-5673.	6.1	198
41	Annealing effects on the optical and structural properties of Al2O3/SiO2 films as UV antireflection coatings on 4H-SiC substrates. Applied Surface Science, 2008, 254, 6410-6415.	6.1	24
42	High responsivity 4H-SiC based metal-semiconductor-metal ultraviolet photodetectors. Science in China Series G: Physics, Mechanics and Astronomy, 2008, 51, 1616-1620.	0.2	6
43	Al2O3/SiO2 films prepared by electron-beam evaporation as UV antireflection coatings on 4H-SiC. Applied Surface Science, 2008, 254, 3045-3048.	6.1	24
44	Effects of annealing on the performance of 4H-SiC metal–semiconductor–metal ultraviolet photodetectors. Materials Science in Semiconductor Processing, 2008, 11, 59-62.	4.0	27
45	High-performance 4H-SiC based metal-semiconductor-metal ultraviolet photodetectors with Al2O3â^•SiO2 films. Applied Physics Letters, 2008, 92, .	3.3	36
46	Visible blind p–i–n ultraviolet photodetector fabricated on 4H-SiC. Microelectronic Engineering, 2006, 83, 104-106.	2.4	20